



TEC variation over Europe during the intense tectonic activity in the area of Arkalochori, Crete, in December 2021.

Contadakis M.E.⁽¹⁾, Arabelos D.N.⁽¹⁾, Pikridas C.⁽¹⁾, Bitharis S.⁽¹⁾, Scordilis, E.⁽²⁾

⁽¹⁾ Department of Geodesy and Surveying, Aristotle University of Thessaloniki, Greece

⁽²⁾ Department of Geophysics, Aristotle University of Thessaloniki, Greece

This paper is one of a series of papers dealing with the investigation of the Lower ionospheric variation on the occasion of an intense tectonic activity. In the present paper, we investigate the TEC variations during the intense seismic activity in the broader area of Arkalochori of Crete on the last quarter of 2021 over Europe. The Total Electron Content (TEC) data are been provided by the Hermes GNSS Network managed by GNSS_QC, AUTH Greece, the HxGN/SmartNet-Greece of Metrica S.A, and the EUREF Network. These data were analysed using Discrete Fourier Analysis in order to investigate the TEC turbulence band content. The results of this investigation indicate that the High-Frequency limit f_o of the ionospheric turbulence content, increases as approaching the occurrence time of the earthquake, pointing to the earthquake epicenter, in accordance to our previous investigations. We conclude that the Lithosphere Atmosphere Ionosphere Coupling, LAIC, mechanism through acoustic or gravity waves could explain this phenomenology.

Keywords: Seismicity, Lower Ionosphere, Ionospheric Turbulence, Brownian Walk, Aegean area.

1.Introduction

It is argued that tectonic activity during the earthquake preparation period produces anomalies at the ground level which subsequently propagate upwards in the troposphere as Acoustic or Standing waves (Miyaki et al. 2002, Hayakawa et al. 2011, Hayakawa 2011, Hayakawa et al. 2018). These Acoustic or Standing waves affect the turbidity of the lower ionosphere, where sporadic Es-layers may appear too, and the turbidity of the F layer. Subsequently, the produced disturbance starts to propagate in the ionosphere's waveguide as gravity wave. The inherent frequencies of the acoustic or gravity wave, range between 0.003Hz (period \approx 5min) and 0.0002Hz (period \approx 100min), which according to Molchanov et al. (2004, 2005) correspond to the frequencies of the turbulent produced by tectonic activity during the earthquake preparation period. During this propagation the higher frequencies are progressively dumped. Thus, observing the frequency content of the ionospheric turbidity we will observe a decrease of the higher limit of the turbidity frequency band.

In this paper we investigate the Lower ionospheric variations from TEC observations during the intense seismic activity of the last quarter of 2021 in the broader area of Arkalochori (Crete, Greece, $34.5^\circ \leq \varphi \leq 35.5^\circ$ N, $25^\circ \leq \lambda \leq 29^\circ$ E). The Total Electron Content (TEC) data are provided by the Hermes GNSS Network managed by GNSS_QC, AUTH Greece, the HxGN/SmartNet-

Greece of Metrica S.A, and the EUREF Network. These data were analysed using Discrete Fourier Analysis in order to investigate the TEC turbulence.

2. Seismotectonic Information of the Study Region

Several studies were carried out in the Hellenic region, focusing on crustal deformation using continuous GPS observations from Greek permanent networks (e.g. McClusky et al. 2000; Nyst and Thatcher 2004; Bitharis 2021). It is widely known that the broader region of Aegean Sea is considered among the most seismically active regions of the Alpine-Himalayan Mountain Belt. The major tectonic feature being responsible and ruling this high seismic activity (figure 1) is the convergence of the Mediterranean and Eurasian tectonic plates with the first subducting under the latter (e.g. Papazachos and Comninakis, 1970, 1971; McKenzie, 1972, 1978; Dewey and Şengör, 1979; Le Pichon and Angelier, 1979, 1981). Important is also the role of the right-lateral North Anatolian Fault Zone, along which the Anatolian plate rotates to the west (e.g. Oral et al., 1995; Papazachos, 1999), as well as of the counter clockwise move of the Apulian microplate to the west (e.g. McKenzie, 1972; Ritsema, 1974) and the S-SW extension of the Aegean microplate (e.g. Papazachos, 1999).

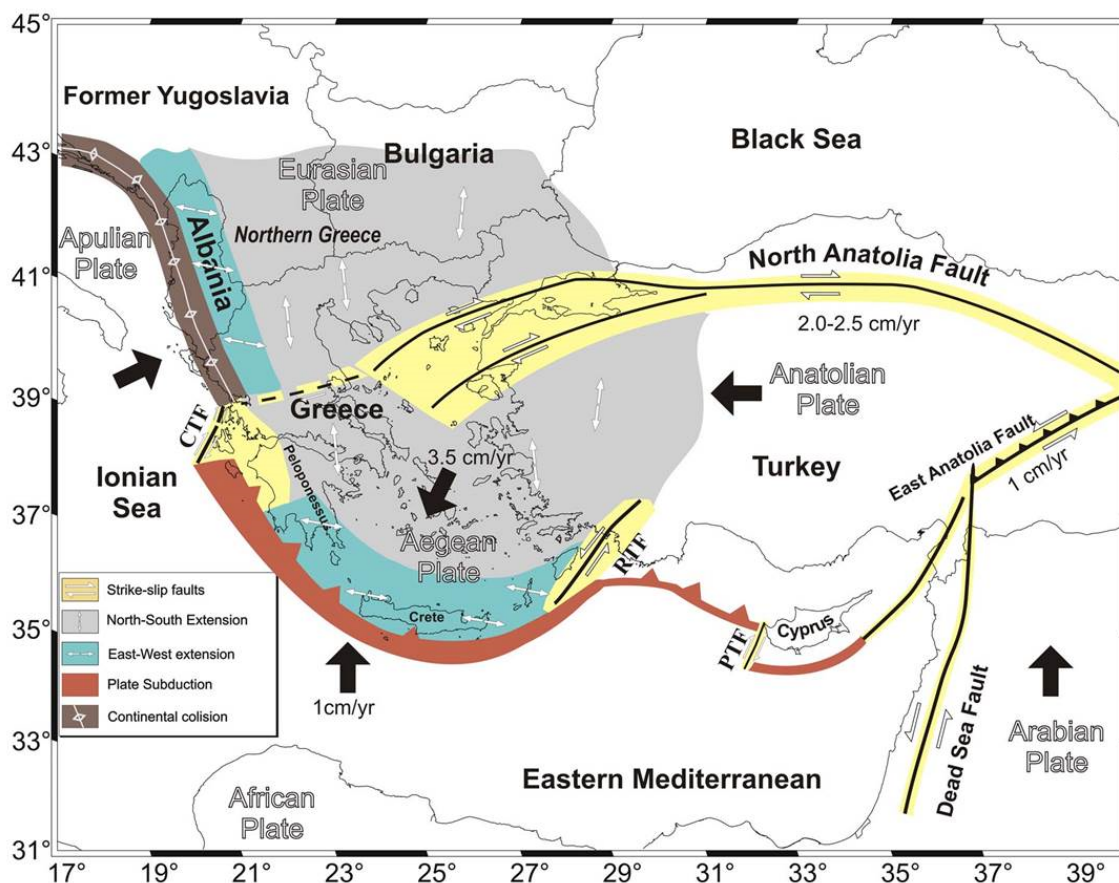


Figure 1. Tectonic regime of Aegean and surroundings (Papazachos et al., 1998).

Four shallow and three intermediate depth earthquakes, of moderate and strong magnitude occurred during the period September-December 2021 in the central and eastern part of the island of Crete and around it. The first, in chronological order, occurred on September 27 (06:17 GMT) with magnitude $M_w=5.9$, in mainland Crete, very close to the village of Arkalochori and was followed the next day (04:48 GMT) by another one of moderate magnitude, $M_w=5.3$. The third and the strongest one with magnitude, $M_w=6.4$ occurred on October 12 (09:24 GMT) at sea, close to the SE cost of Crete. Its strongest aftershock of magnitude 5.6 occurred on December 26. It is worth noting the three events of intermediate depth (focal depths 60-80km) that also took place south and east of Crete on October 19 and December 29 with magnitudes $M_w=5.2-5.9$. Table 1 provides information on the focal parameters of the above seven shocks while figure 2 shows a map with the epicenters of the strongest events ($M \geq 4.0$) of this excitation.

Table 1. Focal parameters of the strong earthquakes that occurred in the region under study during September-December 2021.

(sources: <http://geophysics.geo.auth.gr/ss/bulletins.html>, <https://www.globalcmt.org>)

Year	Date	Origin Time	Latitude (°N)	Longitude (°E)	Depth (km)	M
2021	September 27	06:17:21	35.161	25.272	9	5.9
2021	September 28	04:48:08	35.137	25.235	10	5.3
2021	October 12	09:24:04	34.890	26.360	11	6.4
2021	October 19	05:32:32	34.745	28.203	60	5.9
2021	December 26	18:59:03	35.255	26.856	5	5.6
2021	December 29	05:08:09	34.778	25.154	74	5.7
2021		16:47:08	34.780	25.161	78	5.2

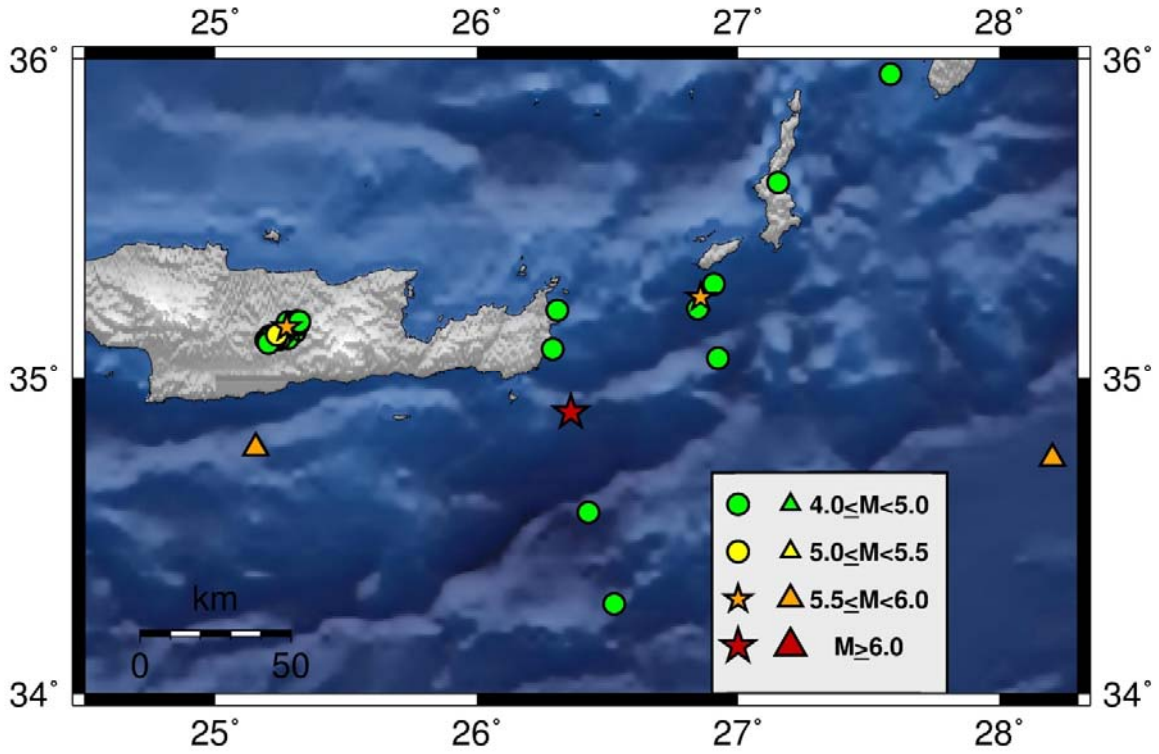


Figure 2. Map of epicenters of the strongest earthquakes ($M \geq 4.0$) that occurred on and around Crete Island during September-December 2021. Triangles stand for the intermediate depth events.

3. TEC Variation Over mid Latitude of Europe

In this study, the TEC values of several GNSS permanent stations were estimated before and after each of the earthquakes under study. The stations are recording satellite data with a 30-sec observation rate. Most of the stations participate to EPN/EUREF network while some of them belong to local permanent networks of Greece such as HermesNet and HxGN/SmartNet-Greece. Stations nearby the geographic latitudes with these earthquakes epicenters were selected.

The TEC values were estimated using the IONosphere Map Exchange (IONEX) Format (Schaer et al.1998) files, where the hourly TEC values from a large network of ten GPS/GNSS stations all over Europe for the test period were estimated.

The processing scenario was applied using the IONEX files that are available at Center for Orbit Determination (CODE). The TEC parameter is modeled with a spherical harmonic expansion up to 15 degree and order 15 referring to a solar-geomagnetic reference frame. The produced ionospheric product is regarded as one of the most precise TEC information.

As it concerns, the TEC estimation for each PRN of the observed satellites included in the selected permanent stations RINEX data, the GPS-TEC software (Seemala and Valladares 2011) was used considering the receiver and inter-channel biases for different satellites in the receiver. The GPS-TEC software was used to derive TEC values from each dual frequency GPS receiver records. Especially, the GPS-TEC software uses the phase and code values for both L1 and L2

GPS frequencies to eliminate the effect of clock errors and tropospheric water vapor to calculate relative values of slant or line-of-sight TEC. TEC values for each observed satellite such as PRN1 (which is studied in detail) are derived with time resolution of one (1) minute. A single-layer approximation is adopted to convert slant TEC (STEC) into vertical (VTEC) values, where ionospheric piercepoint is considered at an altitude of 350 km above the earth's surface.

For the purposes of our investigation we analyze the variations of TEC over the broader area of Mediterranean before and during the seismic activity of the last quarter of 2021 in the broader area of Arkalochori ($34.5^{\circ} \leq \varphi \leq 35.5^{\circ} \text{ N}, 25^{\circ} \leq \lambda \leq 29^{\circ} \text{ E}$). Thus, we use the TEC estimations from EUREF stations of distances ranging from 0 km to 2030.1km from active areas, for the time period from 12/09/2021 to 04/01/2022. The selected GPS stations have about the same latitude and are expected to be affected equally from the Equatorial Anomaly as well as from the Auroral storms.

Table 2. Distance of GPS stations from the epicenter of the earthquake of Arkalochori

GPS Station	Longitude (°E)	Latitude (°N)	Epicentral distance (km)
ARKL (Greece)	25.260000	35.252000	0.00
AUT1(Greece)	22.944230	40.641282	620.5
ISTA(Turkey)	28.979870	41.016791	690.4
ORID(NorthMacedonia)	20.801771	41.123657	721.4
ANKR (Turkey)	32.759000	39.888000	728.1
MATE(Italy)	16.604398	40.667598	845.5
TLSE(France)	1.444209	43.606979	1877.7
YEBE(Spain)	-3.111166	40.533649	2030.1
ZECK(Russia)	41.585293	43.857071	1.4723

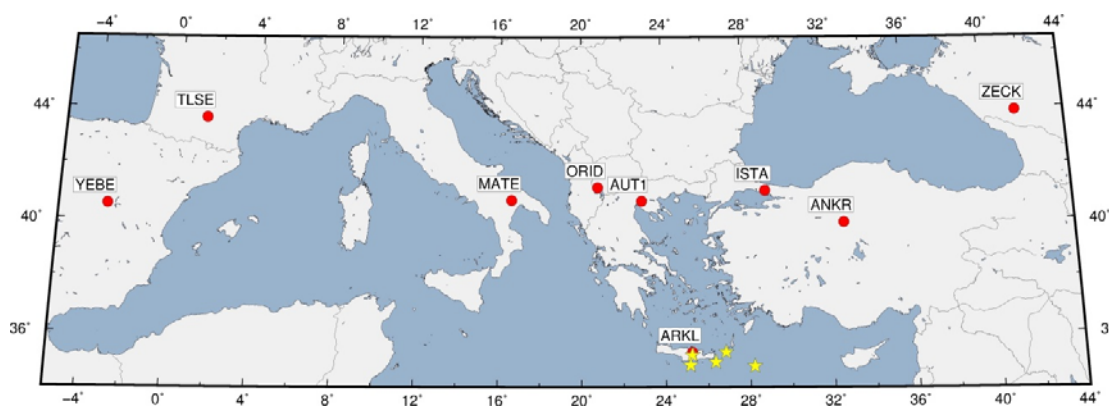


Figure 3. The 9 GPS stations (red circles) and the epicenters of the strongest earthquakes (yellow stars).

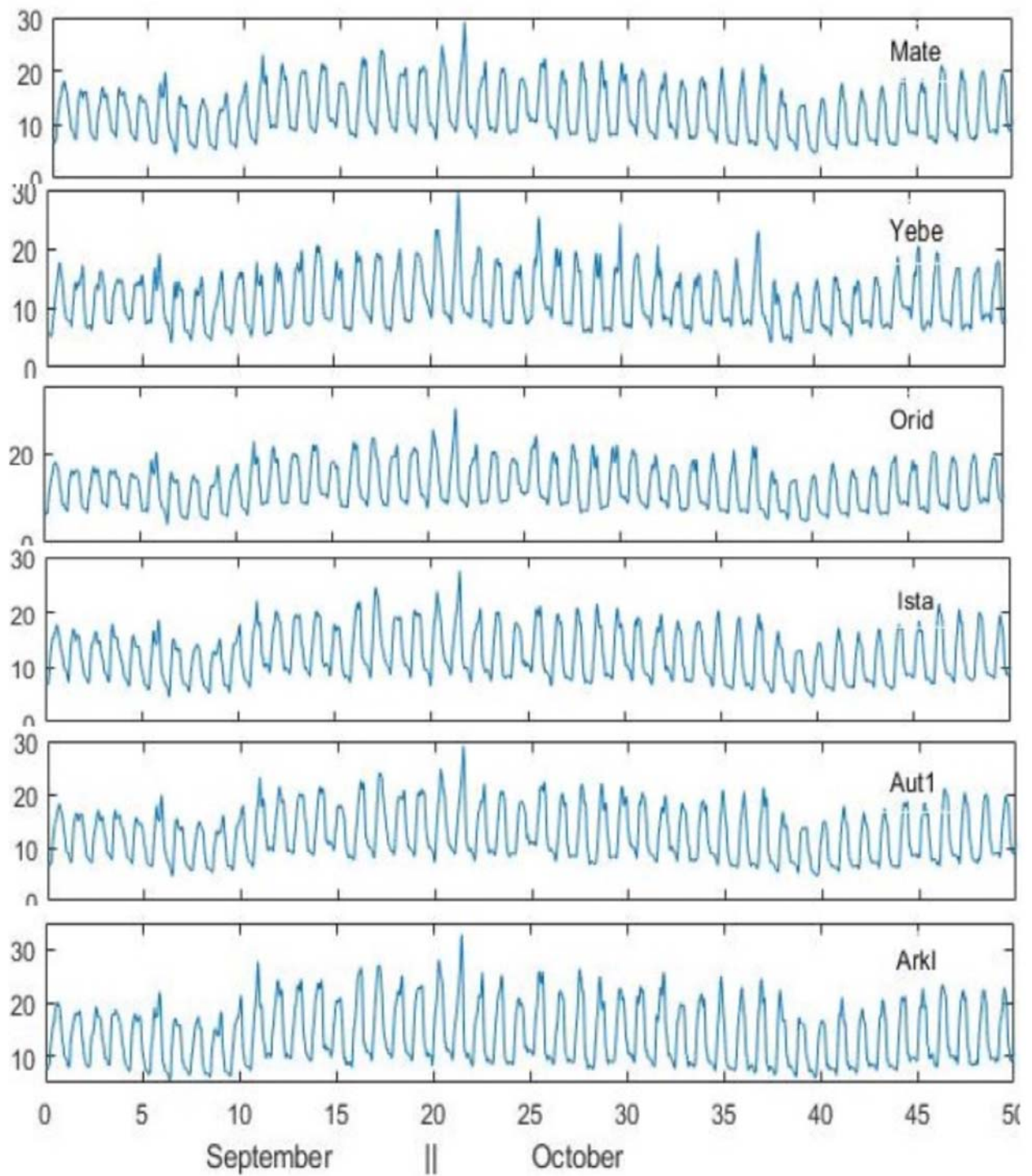


Figure 4. TEC variation over selected GPS stations during September-October of 2021 (abscissa in TECU).

Table 2 displays information about the 9 GPS stations while Figure 3 displays their locations as well as the epicenters of the 6 main events. Figure 4 displays the TEC variation over six selected GPS stations during September and October of 2020.

4. Geomagnetic and Solar Activity Indices

The variations of the geomagnetic field were followed by the Dst-index and the planetary-kp three hour indices quoted from the site of the Space Magnetism Faculty of Science, Kyoto University (<http://swdcwww.kugi.kyoto-u.ac.jp/index.html>) for the time period of our data (Figure 5 presents the Dst-index variations during October 2021).

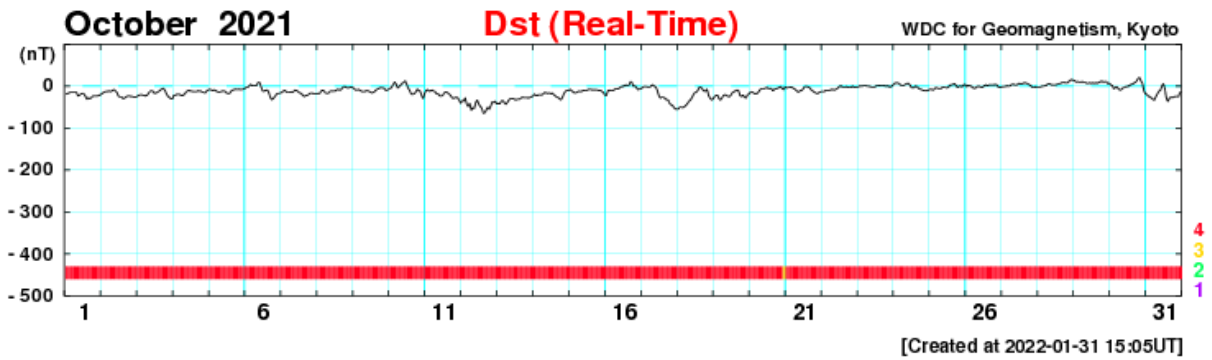


Figure 5. Dst-index variation during October, 2021.

In addition, the solar activity is very low, as it is expected, since October 2020 is at the beginning of the solar activity cycle.

5. Data Process

The Power Spectrum of TEC variations will provide information on the frequency content of them. Apart of the well-known and well expressed tidal variations, for which the reliability of their identification can be easily inferred by statistical tests, small amplitude space-temporal transient variations cannot have any reliable identification by means of a statistical test. Nevertheless looking at the logarithmic power spectrum, we can recognize from the slope of the diagram whether the contributed variations to the spectrum are random or periodical. If they are random the slope will be 0, which corresponds to the white noise, or -2 which corresponds to the Brownian walk noise, otherwise the slope will be different, the so called Fractal Brownian walk noise (Turcotte, 1997). This means that we can trace the presence of periodical variations in the logarithmic power spectrum of TEC variations. As an example, Figure 6 displays the logarithmic power spectrum of TEC variations over the GPS station of Arkalochori on 12 of October 2021. It is seen that the slope of the diagram up to $\log(f_o)=-3.85$ is $b=-2$ (Brownian walk noise) and from $\log(f_o)<-3.85$ (fractal Brownian walk noise). This means that, for frequencies higher than $f_o=\exp(-3.85)$, the TEC variation is random noise. On the contrary, the variation of TEC for lower frequencies contains non-random variations, i.e. turbulent. So we conclude that the upper limit of the turbulent band is $f_o=\exp(-3.85)=0.0213\text{cycl}/(\text{min})\Rightarrow 709.32\mu\text{Hz}$. Or, equivalently, the lower period limit P_o of the contained turbulent is 23.4965 minutes. (It should be noted that the sampling rate is half minute).

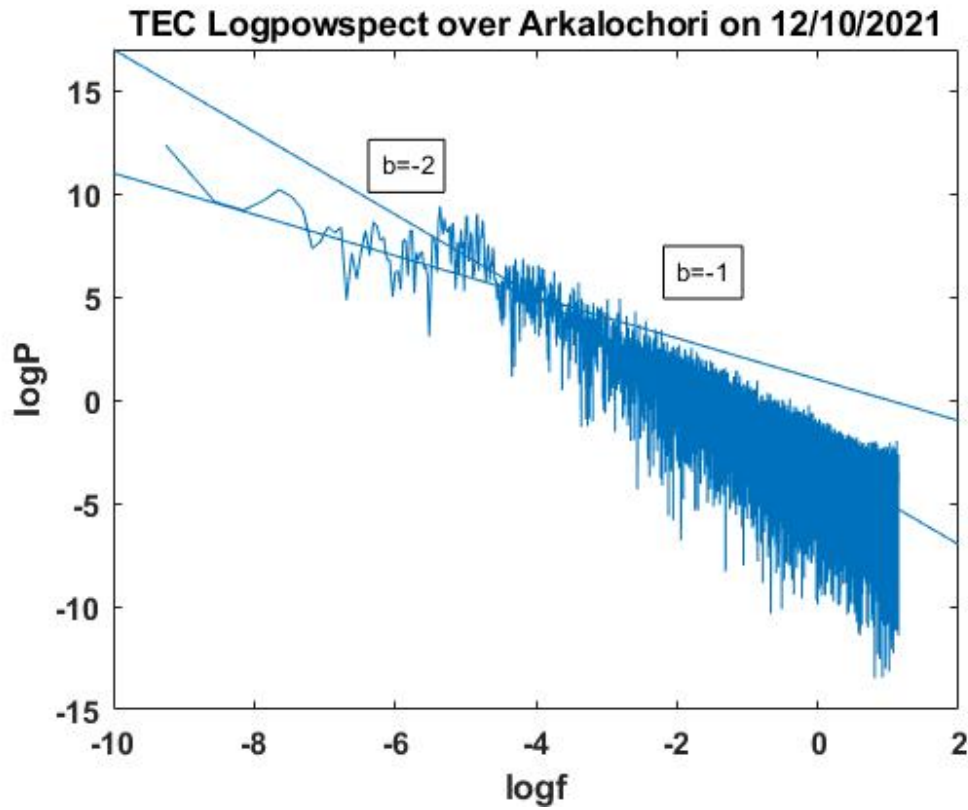


Figure 6. Logarithmic power spectrum of TEC variations over Atkalochori on 12 October 2021.

6. Results

Figures 7 and 8 display the variation of the TEC turbulence frequency band upper limit f_o with time, in days, from the Arkalochori main shock of 12/10/2020, while Figure 9 displays the variation of the TEC turbulence frequency band upper limit f_o with epicentral distance, in km, from the Arkalochori main shock. Figures 10 and 11 display the respective variation of the period lower limit P_o with time and epicentral distance respectively, from the Arkalochori main shock. It is shown that a strong dependence of the upper frequency f_o limit (lower period limit P_o) of the ionospheric turbulent band content with time and with epicentral distance is observed. In particular, the closer in time or in space to the active area the higher frequency f_o limit/lower period P_o , is. The observed frequencies (and the respective periods) are in the range of the observed Acoustic Gravity Waves on the occasions of strong earthquakes, which correspond to periods of 30 to 100 min (Molchanov et al., 2004; Molchanov et al., 2005) or 20 to 80 min (Horie et al., 2007).

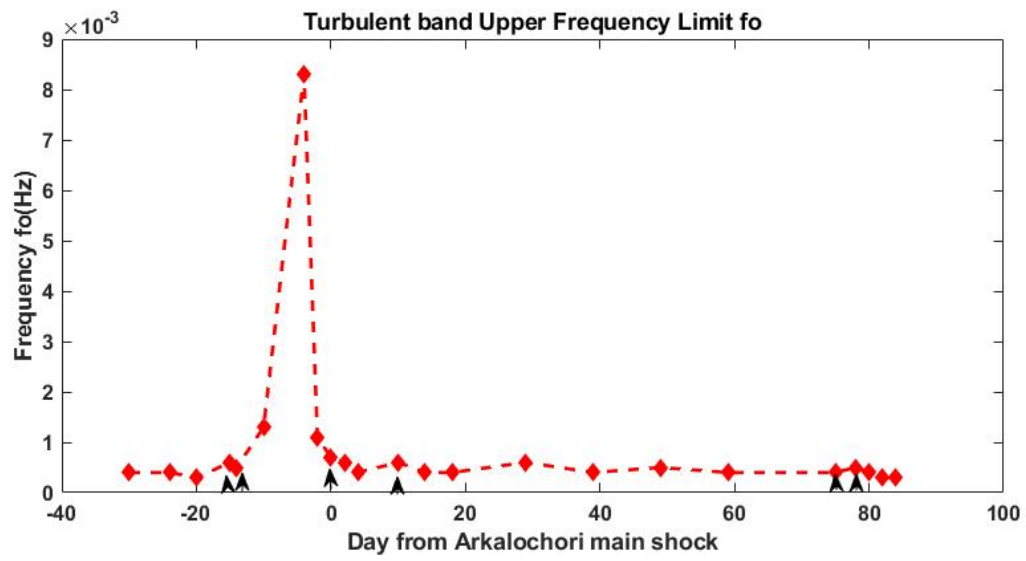


Figure 7. TEC turbulence band upper limit f_o versus time distance from Arkalochori main shock

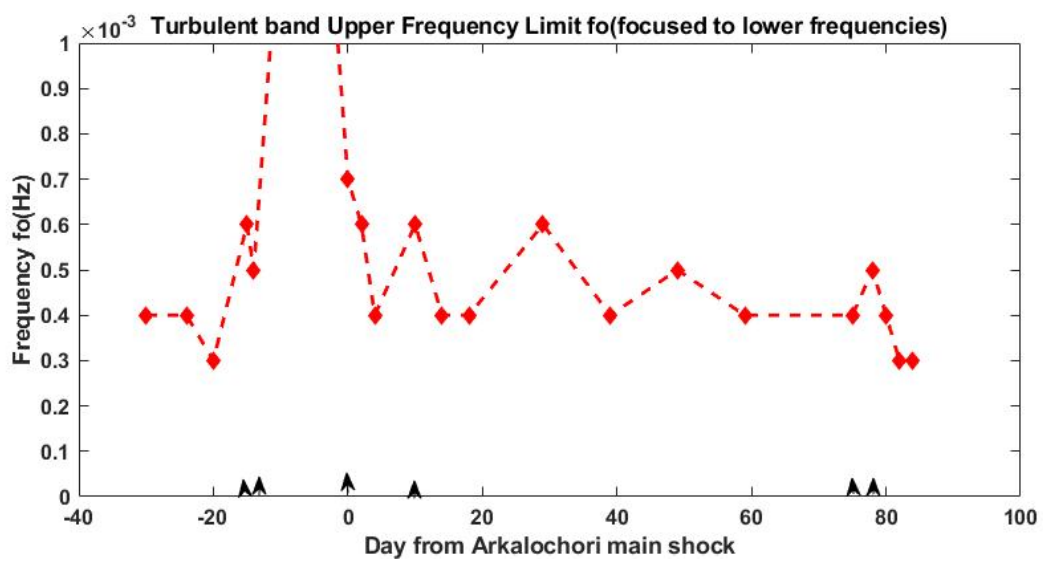


Figure 8. TEC turbulence band upper limit f_o versus time distance from Arkalochori main shock (focused to lower frequencies).

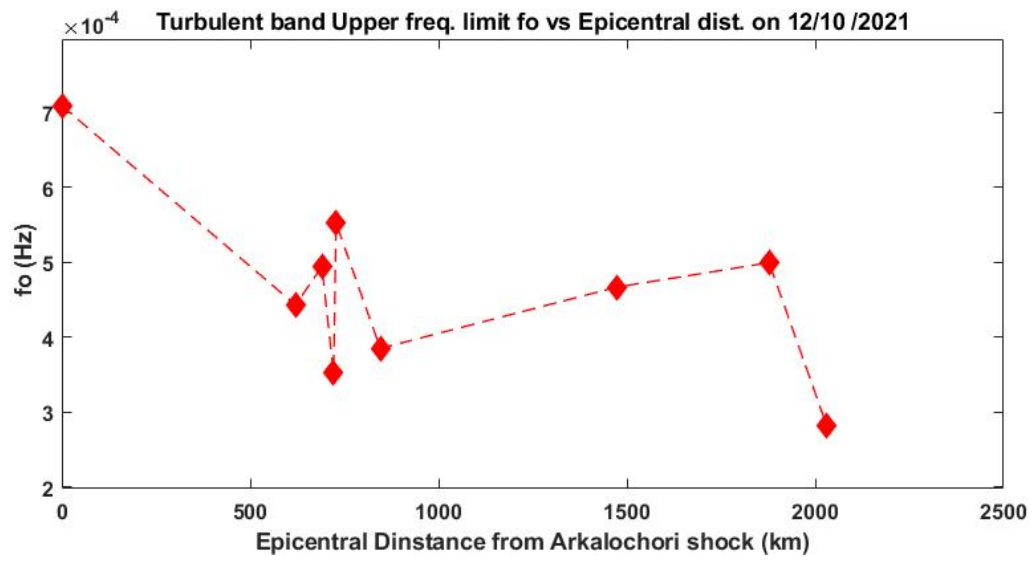


Figure 9. TEC turbulence band upper limit f_o versus epicentral distance from Arkalochori main shock area.

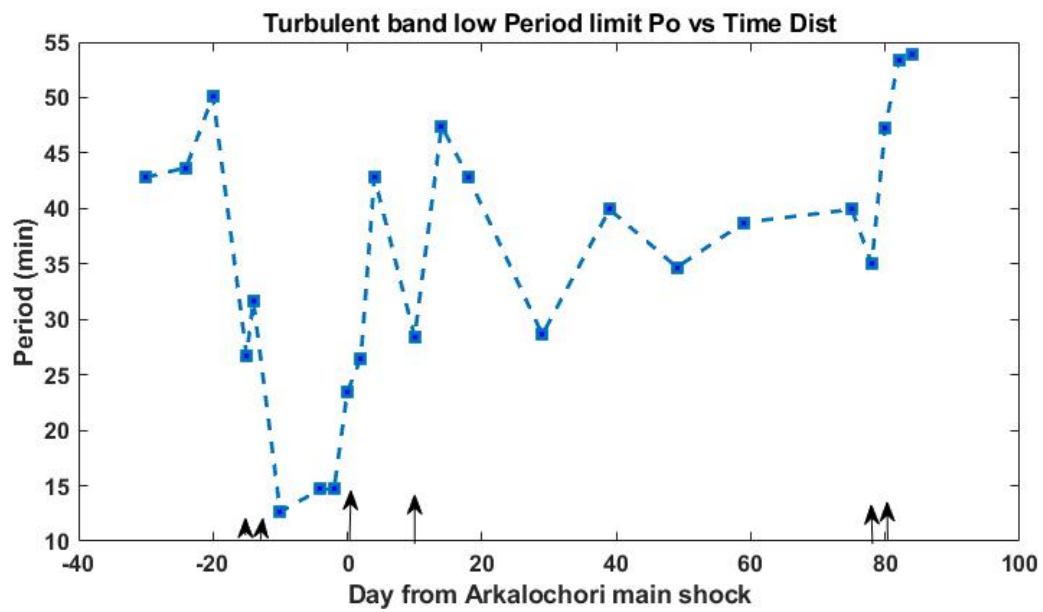


Figure 10. TEC turbulence band lower period limit P_o versus time distance from Arkalochori main shock

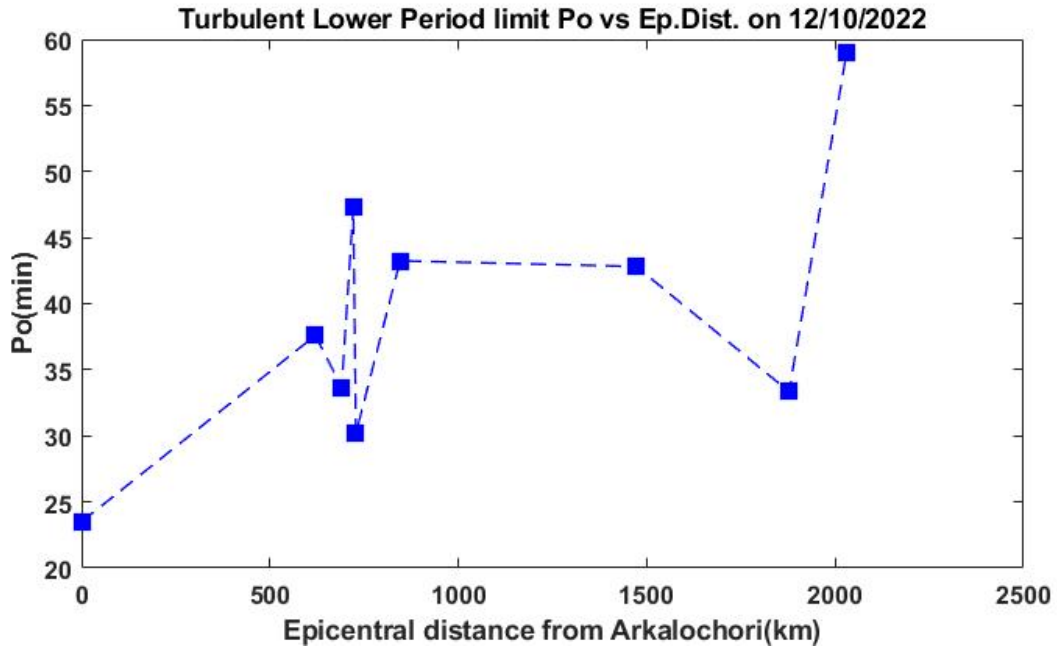


Figure 11. TEC turbulence band lower period limit P_o versus epicentral distance from Arkalochori main shock area.

Hobara et al. (2005) in a study on the ionospheric turbulence in low latitudes concluded that the attribution of the turbulence to earthquake process and not to other sources, i.e. solar activity, storms etc. is not conclusive. Nevertheless in our case, the steady monotonic, time and space, convergence of the frequency band upper limit f_o increment, to the occurrence of the examined strong earthquakes is a strong indication that the observed turbulence is generated by the respective earthquake preparation process.

The qualitative explanation of this phenomenology can be offered on the basis of the Lithosphere Atmosphere Ionosphere Coupling, LAIC: Tectonic activity during the earthquake preparation period produces anomalies at the ground level which propagate upwards in the troposphere as acoustic or standing gravity waves (Hayakawa et al., 2011; Hayakawa, 2011). These acoustic or gravity waves affect both, the turbulence of the lower ionosphere, where sporadic Es-layers may appear too (Liperovsky et al., 2005) and the turbulence of the F-layer. Subsequently, the produced disturbance starts to propagate in the ionosphere's waveguide as gravity wave and the inherent frequencies of the acoustic or gravity waves can be traced on TEC variations [i.e. the frequencies between 0.003Hz (period 5min) and 0.0002Hz (period 100min)], which, according to Molchanov et al. (2004, 2005) and Horie et al. (2007), correspond to the frequencies of the turbulent induced by the LAIC coupling process to the ionosphere. As we move far from the disturbed point, in time or in space, the higher frequencies (shorter wavelength) variations are progressively attenuated.

7. Conclusions

The results of this investigation indicate that the High-Frequency limit f_o of the ionospheric turbulence content, increases as we approach, in time and in space, the point of the occurrence of the earthquake, pointing to the earthquake epicenter, in accordance to our previous investigations

(Contadakis et al., 2015; Scordilis et al., 2020). We conclude that the LAIC mechanism through acoustic or gravity waves could explain this phenomenology.

References

- Bitharis S (2021): Study of the geodynamic field in Greece using modern satellite geodetic methods. *PhD Thesis*, School of Rural and Surveying Engineering, Aristotle University of Thessaloniki, Greece.
- Contadakis, M. E., Arabelos, D.N., Vergos, G., Spatalas, S. D., Scordilis, E.M., (2015). TEC variations over the Mediterranean before and during the strong earthquake (M=6.5) of 12th October 2013 in Crete, Greece, *Physics and Chemistry of the Earth*, Volume 85, p. 9-16.
- Dewey, J. F., and A. M. C. Sengör (1979). Aegean and surrounding regions: complex multiplate and continuum tectonics in a convergent zone, *Geol. Soc. Am. Bull.*, 90, 84–92.
- Hayakawa, M. (2011). On the fluctuation spectra of seismo-electromagnetic phenomena, *Nat. Hazards Earth Syst. Sci.*, 11, 301-308.
- Hayakawa, M., Kasahara, Y., Nakamura, T., Hobara, Y. Rozhnoi, A., Solovieva, M., Molchanov, O.A. and Korepanov, V. (2011). Atmospheric gravity waves as a possible candidate for seismo-ionospheric perturbations, *J. Atmos. Electr.*, 32, 3, 129-140.
- Hayakawa, M., Asano, T., Rozhnoi, A. and Solovieva, M. (2018). Very-low- and low-frequency sounding of ionospheric perturbations and possible association with earthquakes, in *“Pre-earthquake Processes: A multidisciplinary approach to earthquake prediction studies”*, Ed. by D. Ouzounov et al., 277-304, AGU Book, Wiley.
- Hobara, Y., Lefeuvre, F., Parrot, M., and Molchanov, O.A., (2005). Low-latitude ionospheric turbulence observed by Aureol-3 satellite, *Annales Geophysicae*, 23, 1259–1270.
- Horie, T., Maekawa, S., Yamauchi, T. and Hayakawa, M. (2007), A possible effect of ionospheric perturbations associated with the Sumatra earthquake, as revealed from subionospheric very-low-frequency (VLF) propagation (NWC-Japan), *International Journal of Remote Sensing*, vol. 28, issue 13, pp. 3133-3139.
- LePichon X. and J. Angelier (1979). The Hellenic arc and trench system: a key to the neotectonic evolution of the eastern Mediterranean area, *Tectonophysics*, 60, 1-42.
- LePichon X. and J. Angelier (1981). The Aegean Sea, *Philos. Trans. Royal Soc. London*, A300, 357-372.
- Liperovsky V.A., Meister C.-V., Liperovskaya E.V., Vasileva N.E., Alimov O. (2005). *Natural Hazard and Earth System Sciences*, Vol. 5, No 1, 59-62.
- McKenzie D.P. (1972). Active tectonics of the Mediterranean region. *Geophys. J. R. Astr. Soc.*, 30, 109-185.
- McKenzie D.P. (1978). Active tectonics of the Alpine-Himalayan belt: the Aegean Sea and surrounding regions, *Geophys. J. R. Astr. Soc.*, 55, 217-254.
- McClusky S, Balassanian S, Barka A, et al (2000). Global Positioning System constraints on plate kinematics and dynamics in the eastern Mediterranean and Caucasus. *J Geophys Res Solid Earth* 105:5695–5719, doi: 10.1029/1999JB900351.
- Miyaki, K., Hayakawa, M., and Molchanov, O.A., (2002). The role of gravity waves in the lithosphere-atmosphere-ionosphere coupling, as revealed from the subionospheric LF propagation, in *“Seismo Electromagnetics: Lithosphere-Atmosphere-Ionosphere Coupling”*, Ed. by M. Hayakawa and O.A. Molchanov, TERRAPUB, Tokyo, 229-232.
- Molchanov, O., Biagi, P.F., Hayakawa, M., Lutikov, A., Yunga, S., Iudin, D., Andreevsky, S., Rozhnoi, A., Surkov, V., Chebrov, V., Gordeev, E., Schekotov, A. and Fedorov, E. (2004).

- Lithosphere-atmosphere-ionosphere coupling as governing mechanism for preseismic short-term events in atmosphere and ionosphere, *Nat. Hazards Earth Syst. Sci.*, 4, 5/6, 757-767.
- Molchanov, O., Schekotov, A., Solovieva, M., Fedorov, E., Gladyshev, V., Gordeev, E., Chebrov, V., Saltykov, D., Sinitsin, V.I., Hattori, K. and Hayakawa, M. (2005). Near seismic effects in ULF fields and seismo-acoustic emission: statistics and explanation, *Nat. Hazards Earth Syst. Sci.*, 5, 1-10.
- Nyst, M. and Thatcher W (2004). New constraints on the active tectonic deformation of the Aegean. *J Geophys Res Solid Earth*. doi: 10.1029/2003JB002830.
- Oral, M.B., Reilinger, R.E., Toksoz, M.N., King R.W., Barka A.A., Kiniki, J. and D. Lenk (1995). Global Positioning System offers evidence of plate motions in Eastern Mediterranean, *EOS*, 76, 9-11.
- Papazachos B.C. and P.E. Comninakis, (1970). Geophysical features of the Greek Island Arc and Eastern Mediterranean Ridge. *Com. Ren. Des Seances de la Conference Reunie a Madrid*, 1969, 16, 74-75.
- Papazachos B.C. and P.E. Comninakis (1971). Geophysical and tectonic features of the Aegean arc. *J. Geophys. Res.*, 76, 8517-8533.
- Papazachos, B.C., E.E. Papadimitriou, A.A. Kiratzi, C.B. Papazachos and E.K. Louvari (1998). Fault plane solutions in the Aegean and the surrounding area and their tectonic implications, *Boll. Geof. Teor. Appl.*, 39, 199-218.
- Papazachos, C.B. (1999). Seismological and GPS evidence for the Aegean-Anatolia interaction. *Geophys. Int. Lett.*, 26, 2653-2656.
- Ritsema, A.R. (1974). The earthquake mechanism in Balkan region. *Inst. Sci. Rep.*, 74, 1-36.
- Schaer, S., Werner, G. and J. Feltens. (1998). IONEX: The ionosphere map exchange format version 1. *Proceedings of the IGS AC workshop*, Darmstadt, Germany. Vol. 9. No. 11.
- Scordilis E.M., Contadakis M.E, Vallianatos F. and Spatalas S., Lower Ionospheric turbulence variations during the intense tectonic activity in Eastern Aegean area, *Annals of Geophysics*, 63, 5, PA544, 2020
- Seemala, G.K., and Valladares, C.E. (2011), Statistics of total electron content depletions observed over the South American continent for the year 2008, *Radio Science*, 46, RS5019, doi:10.1029/2011RS004722.
- Turcotte D.L. (1997). Fractal and Chaos in Geology and Geophysics (2nd Edition), *Cambridge University Press*, Cambridge U. K.